ЖЭТФ, 2013, том 143, вып. 1, стр. 158–165

DISTORTIONS OF THE COULOMB BLOCKADE CONDUCTANCE LINE IN SCANNING GATE MEASUREMENTS OF InAs NANOWIRE BASED QUANTUM DOTS

A. A. Zhukov [a*], ***Ch. Volk*** [b,c], ***A. Winden*** [b,c], ***H. Hardtdegen*** [b,c], ***Th. Schäpers*** [b,c,d]

[a] *Institute of Solid State Physics, Russian Academy of Sciences*
142432, Chernogolovka, Moscow Region, Russia

[b] *Peter Grünberg Institut (PGI-9), Forschungszentrum Jülich*
52425, Jülich, Germany

[c] *JARA-Fundamentals of Future Information Technology, Forschungszentrum Jülich*
52425, Jülich, Germany

[d] *II. Physikalisches Institut, RWTH Aachen Universität*
52056, Aachen, Germany

Received February 28, 2012

We performed measurements at helium temperatures of the electronic transport in the linear regime in an InAs quantum wire in the presence of a charged tip of an atomic force microscope (AFM) at low electron concentration. We show that at certain concentration of electrons, only two closely placed quantum dots, both in the Coulomb blockade regime, govern conductance of the whole wire. Under this condition, two types of peculiarities — wobbling and splitting — arise in the behavior of the lines of the conductance peaks of Coulomb blockade. These peculiarities are measured in quantum-wire-based structures for the first time. We explain both peculiarities as an interplay of the conductance of two quantum dots present in the wire. Detailed modeling of wobbling behavior made in the framework of the orthodox theory of Coulomb blockade demonstrates good agreement with the obtained experimental data.

DOI: 10.7868/S0044451013010158

1. INTRODUCTION

During the last decade, measurements of the conductance of low-dimensional systems using a charged AFM tip as a mobile gate (scanning gate microscopy measurements or SGM measurements) proved to be a powerful and efficient method. Using this technique, different types of micro- and nanostructures have been investigated such as quantum point contacts [1–3], quantum rings [4], and quantum dots based on heterojunctions [5–7], graphene [8, 9], carbon nanotubes [10–12], and InAs nanowires [13, 14].

While experiments on carbon nanotubes did not result in essentially new effects (the potential profile along the nanotubes was measured in [10] and the stability of the 4-fold energy level degeneracy against long-range Coulomb potential disturbances was confirmed in [12]), several unexpected experimental results on quantum dots based on graphene have been obtained [8, 9]. The presence of bound states in the contact constriction regions was shown and, additionally, wobbling and splitting of the Coulomb blockade conductance line [8, 9] were observed. While the splitting of the Coulomb blockade conductance lines was explained as the crossing of the state of two neighboring dots [8, 9], the mechanism of the wobbling of these lines remains unclear.

One of the problems to be solved before any speculations on the physical mechanism of the observed effect is the correct interpretation of the results of SGM measurements. The initial statement that SGM experimental results are intuitively clear is not always correct; for example, both splitting gates served to form the structure under investigation [15] and charged dielectric dirt on the conductive tip [6] result in additional artifacts

*E-mail: azhukov@issp.ac.ru

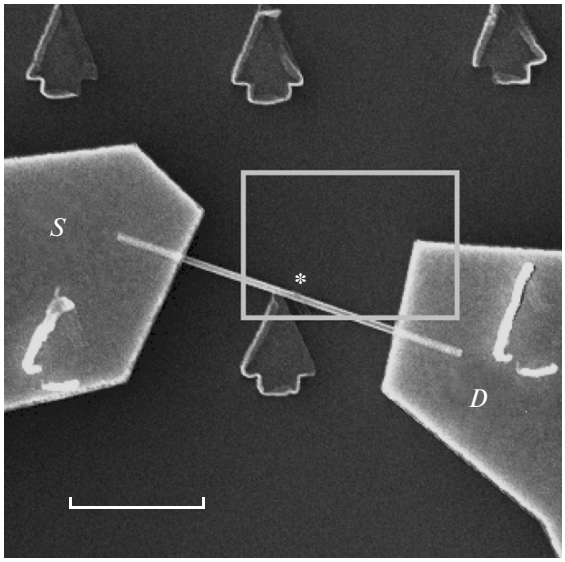

Fig. 1. Scanning electron microscope image of the InAs wire. The source and drain contact pads are marked by "S" and "D". The scale bar corresponds to 2 μm. The rectangle represents the area of the scanning gate measurements at helium temperature. The position of the tip during the transport measurements (V_{SD} vs V_{BG}) is marked by an asterisk

in the SGM experimental data. Thus, not only the explicitly interpreted experimental SGM data but also additional simulations and model calculations of the SGM measurements are absolutely necessary [6, 15].

In this paper, we present SGM experimental results measured in an InAs quantum wire at helium temperature. Wobbling and splitting of the Coulomb blockade conductive lines are observed. The obtained experimental results are interpreted within a model that involves two quantum dots connected in series. Calculations focused on the wobbling behavior of SGM scans in the framework of the orthodox theory of Coulomb blockade for different mutual capacitive couplings between two dots are also presented.

2. EXPERIMENTAL

The InAs undoped nanowire used in our experiment was grown by selective-area metal–organic vapor-phase epitaxy [16]. The wire diameter is 100 nm. For our transport measurements, the wire was transferred to an n-type doped Si (100) wafer covered by a 100 nm thick SiO_2 insulating layer. The doped silicon substrate serves as the back gate. The evaporated Ti/Au contacts to the wire and the markers of the search pattern were defined by electron-beam lithography. The distance between the contacts is 3.5 μm. A scanning electron microscopy image of the sample under investigation is presented in Fig. 1; the rectangle marks the area of the scanning gate measurements.

The measurements were performed at $T = 4.2$ K. The charged tip of a home-built scanning probe microscope [17] is used as a mobile gate during scanning gate imaging measurements. We left the tip 300 nm above the SiO_2 surface, in order to eliminate any mechanical or electrical contact of the tip with the InAs wire or metallic contacts. All scanning gate measurements were performed keeping the potential of the scanning probe microscope tip (V_t) and the backgate voltage (V_{BG}) constant. The electrical circuit of the scanning gate imaging measurements is presented elsewhere [12].

3. EXPERIMENTAL RESULTS

The conductance of the wire during the scan and the conductance as a function of the source-to-drain voltage (V_{SD}) and V_{BG} is measured in a two-terminal scheme by using the standard lock-in technique. Here, a driving AC voltage with the amplitude $V_{AC} = 0.1$ mV at a frequency of 231 Hz is applied while the current is measured with a current amplifier.

The wire conductance map as a function of V_{SD} and V_{BG} is presented in Fig. 2. The tip voltage $V_t = 4$ V is applied during this experiment. The position of the tip is marked by an asterisk in Fig. 1. The experimental data revealed a quite complex Coulomb diamond structure, which is typical for system of two or more quantum dots connected in series [18, 19, 13]. Formation of dots in the quantum wire occurs because of defects in the wire crystal structure.

Figure 3 presents the set of the scanning gate measurements performed with the constant tip voltage $V_t = 4$ V. Here, the backgate voltages were increased successively from $V_{BG} = 0.89$ V (Fig. 3*a*) in steps of 10 mV to the final value $V_{BG} = 1.06$ V (Fig. 3*r*). This set of SGM measurements demonstrates the formation of two quantum dots in the InAs wire connected in series. Some asymmetry of the scanning gate imaging pictures is due to the nonperfect shape of the AFM tip. The centers of the two observed dots are placed approximately 350 nm apart, as can be seen in the enlarged scan shown in Fig. 4*a*.

The set of experiments presented in Fig. 3 was intended to reveal the formation of the double-dot structure in the most explicit way and to eliminate any suspicions about the possibility of a more complex structure realized in the InAs nanowire in the relevant range of backgate voltages. With increasing the backgate

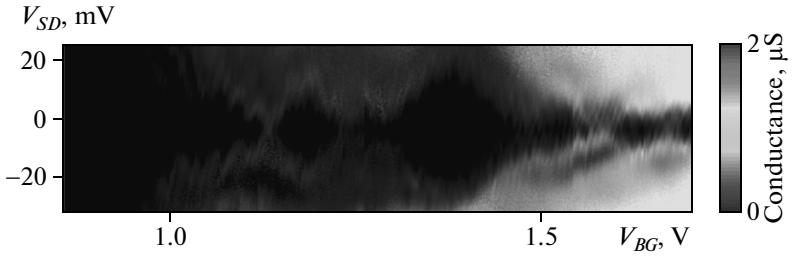

Fig. 2. Conductance map measured at 4.2 K as a function of the source-to-drain voltage and backgate voltage. The double Coulomb blockade pattern reveals the presence of at least two quantum dots connected in series. The applied tip voltage is $V_t = 4$ V, the tip position is marked by the asterisk in Fig. 1

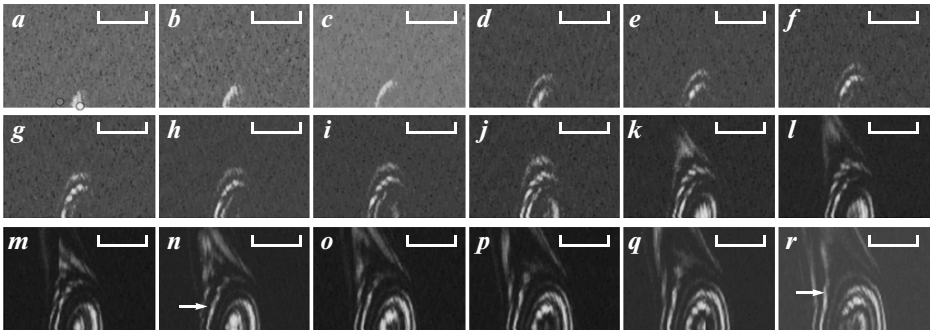

Fig. 3. Series of scanning gate measurements of the InAs nanowire measured from $V_{BG} = 0.89$ V to 1.06 V in steps of 10 mV. The tip voltage is kept constant at 4 V. Brighter areas correspond to a higher conductance. In (a), the positions of dots 1 and 2 are respectively marked with grey and white circles. Coulomb blockade conductance lines with wobbling (in (n) and (r)) are marked with arrows. The scale bar corresponds to 1 μm for all images

voltage, dot 1 (the left one in Fig. 3) starts to be filled with electrons, then dot 2 (the right one) starts to be occupied with electrons. As dot 2 is filled with electrons, the resistance of the InAs nanowire decreases below 100 MΩ. In Fig. 3n, the wobbling of the Coulomb blockade conductive line of dot 2 occurs for the first time at $V_{BG} = 1.02$ V. Subsequently, with increasing the backgate voltage, the wobbling is suppressed (Fig. 3o–q) and then revives at $V_{BG} = 1.06$ V, as can be seen in Fig. 3r. To reveal the interplay of the conductance of both dots, Fig. 4a reproduces Fig. 3n with additional dashed lines corresponding to the lines of conductance minimums of dot 1 (grey) and lines of conductance peaks of dot 2 (white).

Figure 4b shows a scanning gate measurement made at $V_t = 4$ V and $V_{BG} = 1.40$ V. It is clearly seen that at the higher backgate voltage, a new feature, the splitting of the Coulomb blockade conductive lines, is observed (marked with arrows) in addition to the wobbling of the Coulomb blockade conductive lines. A similar behavior of the Coulomb blockade conductance lines was observed in a graphene-based quantum dot [9]. In [9], the splitting of the Coulomb blockade conductance lines was interpreted as the crossing of the state of two neighboring dots with mutual Coulomb interaction, but the wobbling of the Coulomb blockade conductance lines was not explained.

4. THEORETICAL SIMULATIONS OF SGM MEASUREMENTS AND DISCUSSION

The main aim of simulations in framework of the orthodox theory of Coulomb blockade is to confirm the statement that the physical mechanism of wobbling is based on the interplay, revealed with SGM of the conductance of two quantum dots connected in series (see Figs. 3 and 4). To show the influence of the parameters of the quantum dots on the SGM presented in Figs. 3n–r, we performed SGM simulations for different widths of the quantum dot energy levels and their mutual Coulomb interactions.

In our calculations, generally speaking, we need to

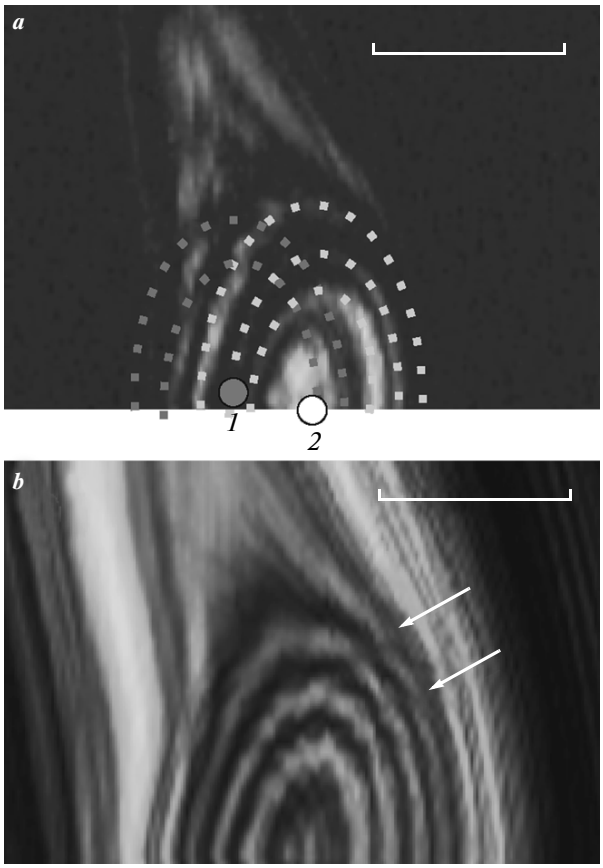

Fig. 4. *a* — A scanning gate measurement of the InAs wire measured at $V_t = 4$ V and $V_{BG} = 1.02$ V (copy of Fig. 3*n*). Grey and white dotted lines are respectively valley and peaks of the Coulomb blockade conductance of dots 1 and 2. The positions of dot 1 and 2 are marked by grey and white dots. *b* — Scanning gate measurement performed at $V_t = 4$ V and $V_{BG} = 1.40$ V. The positions of the splitting of the Coulomb conductance lines are marked by arrows. The scale bar corresponds to 1 μm in both images

take into account the dot-1(2)-to-backgate capacitance $C_{1(2)BG}$, the dot-1(2)-to-tip capacitance $C_{1(2)t}$, the mutual capacitance of the dots C_m, and the capacitance of the dot 1(2) to the left(right) contact $C_{L(R)}$. The charging energy of the individual dot and the mutual charging energy of both dots can then be expressed as [20]

$$E_{C1} = \frac{e^2}{C_1}\left(1 - \frac{C_m^2}{C_1 C_2}\right)^{-1},$$

$$E_{C2} = \frac{e^2}{C_2}\left(1 - \frac{C_m^2}{C_1 C_2}\right)^{-1},$$

$$E_{Cm} = \frac{e^2}{C_m}\left(\frac{C_m^2}{C_1 C_2} - 1\right)^{-1},$$

where

$$C_{1(2)} = C_{L(R)} + C_{1(2)BG} + C_{1(2)t} + C_m$$

is the sum of all capacitances attached to dot 1(2). Taking into account that

$$C_{1(2)t} \equiv C_t(r_{1(2)}) \ll C_{1(2)BG}$$

for any tip-to-dot-1(2) distance ($r_{1(2)}$) because the thickness of the SiO_2 layer is 100 nm and the tip is 300 nm above the sample surface during scanning gate measurements, the expression of the total capacitance of dot 1(2) can be simplified to the form

$$C_{1(2)} = C_{L(R)} + C_{1(2)BG} + C_m.$$

In our calculations, we assume that the lever arm for charging the nanowire by the backgate voltage is constant,

$$\alpha = \frac{C_{1(2)BG}}{C_{1(2)}} = \frac{1}{4}.$$

This value seems to be reasonable taking into account that the voltage drop across a single quantum dot is two times smaller than the applied source-to-drain voltage (see Fig. 2). For simplicity, we set

$$C_{1BG} = C_{2BG}, \quad C_1 = C_2.$$

The positions of the bottom of dots 1 and 2 are set to $\mu_{01} = -0.05$ eV and $\mu_{02} = -0.15$ eV.

We used the standard formulas for the electrochemical potential in quantum dots [20]:

$$\mu_1(N_1, N_2) \equiv U(N_1, N_2) - U(N_1 - 1, N_2) = \\ = \left(N_1 - \frac{1}{2}\right) E_{C1} + N_2 E_{Cm} - \\ - \frac{1}{|e|}(C_{1BG} V_{BG} E_{C1} + C_{2BG} V_{BG} E_{Cm} + \\ + C_{1t} V_t E_{C1} + C_{2t} V_t E_{Cm}) \quad (1)$$

and

$$\mu_2(N_1, N_2) \equiv U(N_1, N_2) - U(N_1, N_2 - 1) = \\ = (N_2 - \frac{1}{2}) E_{C2} + N_1 E_{Cm} - \\ - \frac{1}{|e|}(C_{2BG} V_{BG} E_{C2} + C_{BG} V_{BG} E_{Cm} + \\ + C_{2t} V_t E_{C2} + C_{1t} V_t E_{Cm}). \quad (2)$$

In our calculations, we set

$$E_{C1} = E_{C2} = 13 \text{ meV}, \quad V_t = 4 \text{ V}.$$

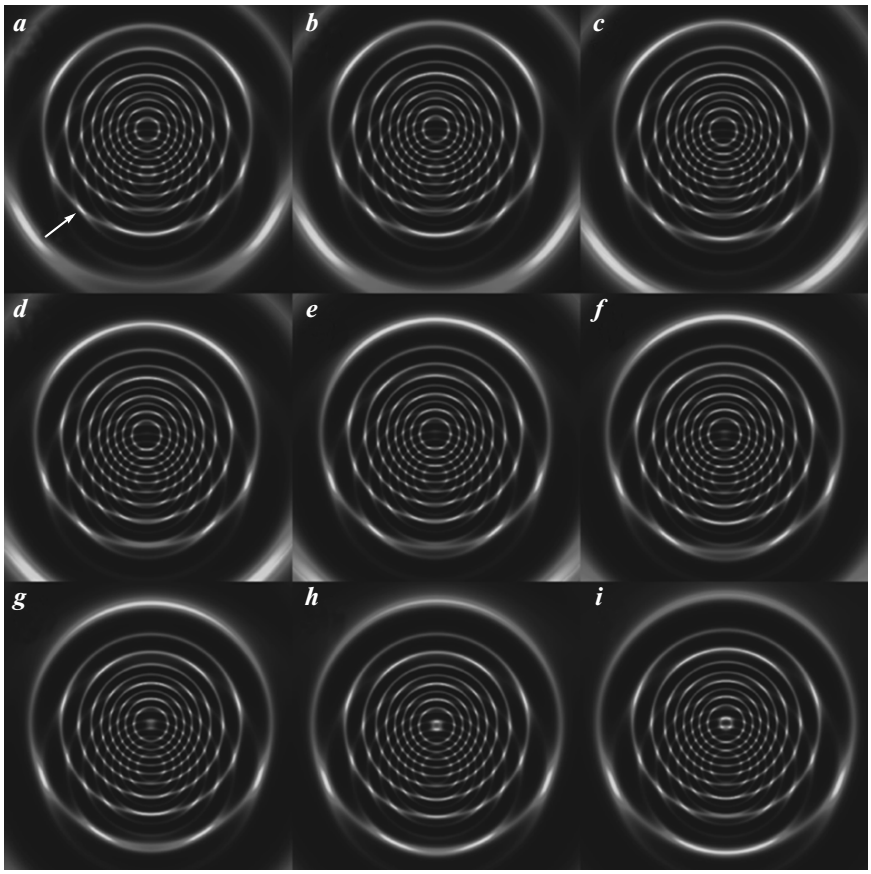

Fig. 5. Series of simulated scanning gate measurements. Simulations are performed for V_t=4 V and for V_{BG} values from -0.184 V to -0.152 V in steps of 4 mV. Other simulation parameters are specified in the text. The outer Coulomb blockade conductance line with wobbling is marked by an arrow

The expression for $C_{1(2)t}$ is included in the form

$$C_{1(2)t}(r) = \frac{2R_t}{\sqrt{\Delta x_{1(2)}^2+\Delta y_{1(2)}^2+\left(z_t+R_t-\dfrac{D_{wire}}{2}\right)^2}} - \frac{2R_t}{\sqrt{\Delta x_{1(2)}^2+\Delta y_{1(2)}^2+\left(z_t+R_t+\dfrac{2\delta z}{\epsilon}+\dfrac{D_{wire}}{2}\right)^2}},$$

where $\Delta x_{1(2)}$ and $\Delta y_{1(2)}$ are the positions of the tip relative to the center of quantum dot 1(2), $R_t = 100$ nm is the tip radius, $D_{wire} = 100$ nm is the nanowire diameter, and $z_t = 300$ nm is the height of the tip above the substrate surface. In our simulations, the quantum dots are placed 300 nm apart of each other.

The conductance through the double-dot system in the linear regime is determined by sequential tunneling through both dots. In our SGM experiment, the widths of the energy levels of the quantum dots are essentially larger than the temperature, and therefore the Lorentz shape broadening of the energy levels can be used [21]. We therefore use the formula

$$I \propto \frac{\Gamma_1^2}{\Gamma_1^2+\mu_1^2}\,\frac{\Gamma_2^2}{\Gamma_2^2+\mu_2^2}$$

for the current through the system, where Γ_1 and Γ_2 are the level widths of dot 1 and 2. The Fermi-level energy is assumed to be zero.

We first performed calculations to illustrate the envelope and the transformation of the wobbling of the conductance peak line of the Coulomb blockade with increasing the backgate voltage. In our simulations, we kept the tip voltage constant, $V_t = 4$ V. The backgate voltage V_{BG} is equal to -0.184 V in Fig. 5*a* and is increased gradually in steps of 4 mV to -0.152 V in Fig. 5*i*. The energy level widths of the quantum dots are $\Gamma_1 = 1$ meV and $\Gamma_2 = 2$ meV.

It is clearly seen that wobbling is most pronounced

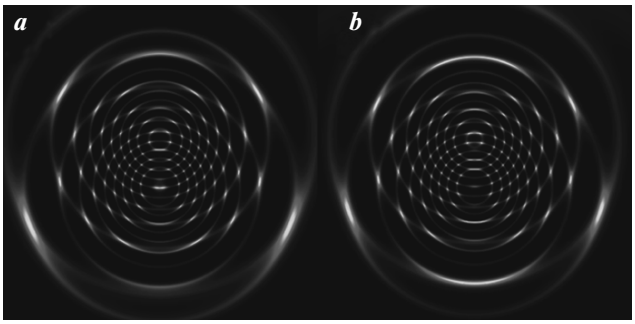

Fig. 6. Two simulated SGM for $V_t = 4$ V and $V_{BG} = -0.184$ V (a) and -0.152 V (b), which are the same as in Fig. 5a and Fig. 5f. The value of level width for both dots is $\Gamma_1 = \Gamma_2 = 1$ meV. No wobbling of the Coulomb conductance peak lines is observed

when the Coulomb blockade conductance peak lines from two dots coincide for quite a long distance (see Fig. 5a,b and Fig. 5h–i) and is smeared at intermediate gate voltages

$$-0.172 \text{ V} \leq V_{BG} \leq -0.164 \text{ V}$$

(Fig. 5d–f). This is similar to the measured experimental data in Fig. 3o–q. To observe the wobbling, it is necessary that the energy level broadening of one of the dots be larger than that of the other. Otherwise, the SGM image is similar to images presented in Fig. 6a and Fig. 6b. Here, the calculations are performed with the same parameters as in Fig. 5a and Fig. 5f, except for the level width, which is the same for both dots $\Gamma_1 = \Gamma_2 = 1$ meV.

Wobbling has been observed previously in a graphene-based quantum dot [9]. The observed feature was interpreted in terms of a particular structure of the quantum confinement of the quantum dot formed by split gates. Based on our simulations, we suggest another explanation of this effect. We suppose the presence of a double quantum dot structure in the system [9, 15]. The second dot may be formed with weakly bound states similar to those in contact constrictions. The conductance peak lines of the Coulomb blockade created by this second open quantum dot can interplay with the conductance peak lines of the closed dot, resulting in the observed wobbling.

Figure 7 shows simulations of the scanning gate measurements for different values of the mutual capacitance C_m or electrostatic coupling energies E_{Cm}. The values of the backgate voltage and tip voltage are kept constant, $V_t = 4$ V and $V_{BG} = 1$ V. The values of the level widths of both dot 1 and dot 2 are $\Gamma_1 = 1$ meV and $\Gamma_2 = 2$ meV. While the value of the electrostatic coupling energy is comparable with the widths of the quantum dot energy levels, the crossing of the Coulomb blockade conductance peak lines occurs similarly to the one observed experimentally (see Ref. [7]). At higher values of the electrostatic coupling energy (see Figs. 7h–i), when E_{Cm} is comparable with $E_{C1(2)}$, a complete redistribution of the Coulomb blockade conductance peak lines occurs in a manner of the formation of a single larger quantum dot, as is expected [20].

It is worth noting that at high values of E_{Cm}, another type of wobbling of the Coulomb blockade conductance peak lines develops (regime II). In this regime, the spatial variation of line wobbling is considerably larger than the line width caused by the energy level broadening as it was obtained in the case of a double dot with no mutual capacitance (see Fig. 3n and Fig. 4r for experimental data and Fig. 5a and Fig. 5f for SGM simulations).

To eliminate artifacts caused by metallic split gates, a double-dot structure formed by local anodic oxidation was investigated in [7]. No wobbling of the Coulomb blockade conductance lines was observed. This result is in good agreement with our simulations: no wobbling is expected while the energy levels widths of both dots are the same (see Fig. 6) and the mutual capacitance energy (E_{Cm}) is larger than the energy level widths (cf. Fig. 7e,f).

5. CONCLUSIONS

In conclusion, we performed scanning gate microscopy measurements of an InAs quantum wire in the linear regime at low electron densities. We show using SGM data that at a certain range of backgate voltages, the wire is split into two quantum dots connected in series. In this regime, wobbling and splitting of the Coulomb blockade conductance peak lines are observed. Both effects are explained as the interplay of the conductance of two quantum dots present in the system. Simulations of the wobbling in the framework of the orthodox theory of Coulomb blockade involved two quantum dots connected in series demonstrate good agreement with the experimentally obtained SGM data.

The same model simulations of scanning gate microscopy measurements are performed for different values of the mutual capacitance of quantum dots. It is found that the wobbling of the Coulomb blockade conductance peak lines occurs in two different regimes.

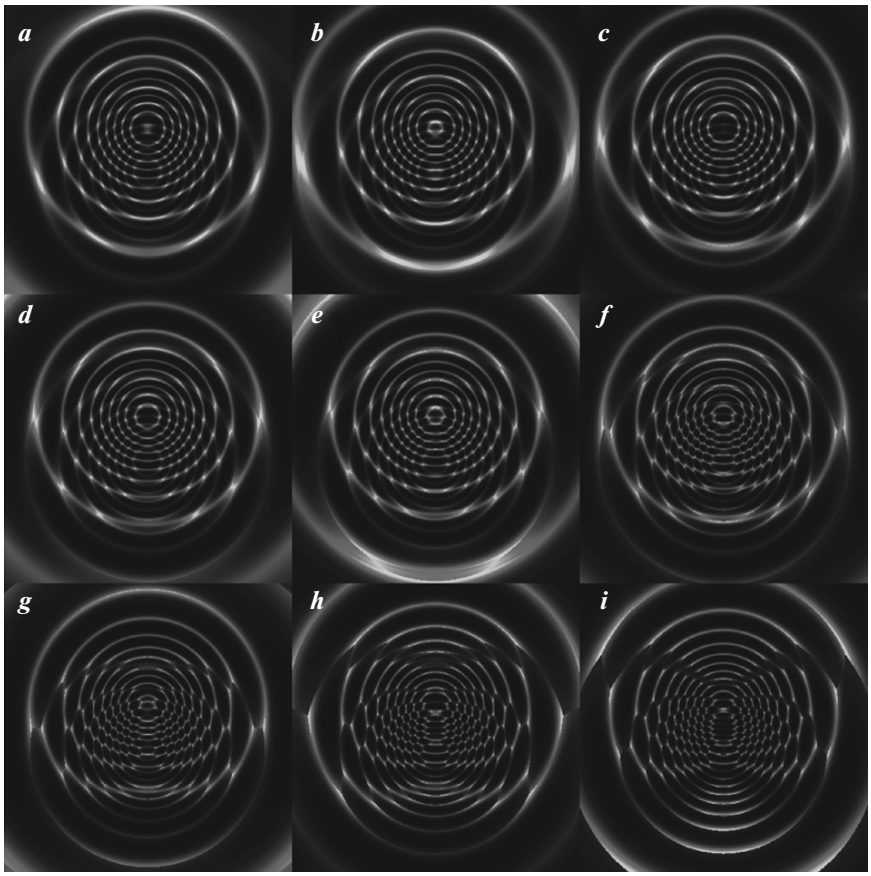

Fig. 7. Set of simulated scanning gate measurements. The simulations are performed for $V_t = 4$ V and $V_{BG} = -0.184$ V. The respective values of mutual capacitance energy E_{Cm} are 0, 0.4, 0.6, 0.8, 1, 2, 3, 4, and 5 meV for (a) through (i). Other calculation parameters are specified in the text. Note that in (i), the wobbling of the Coulomb conductance peak lines in a zig-zag manner revives (regime II)

The first regime is realized at the energy of the mutual capacitance smaller than the energy level widths and the second occurs at a value of the mutual capacitance of the order of the total capacitance of the dots.

This work is supported by the Russian Foundation for Basic Research (grants №№ 10-02-00198-a, 11-02-12071-ofi-m-2011, 12-02-00272-a), programs of the Russian Academy of Sciences, the Program for Support of Leading Scientific Schools, and by the International Bureau of the German Federal Ministry of Education and Research within the project RUS 09/052.

REFERENCES

1. M. A. Topinka, B. J. LeRoy, S. E. J. Shaw, E. J. Heller, R. M. Westervelt, K. D. Maranowski, and A. C. Gossard, Science **289**, 2323 (2000).

2. M. A. Topinka, B. J. LeRoy, R. M. Westervelt, S. E. J. Shaw, R. Fleischmann, E. J. Heller, K. D. Maranowski, and A. C. Gossard, Nature **410**, 183 (2001).

3. S. Schnez, C. Rössler, T. Ihn, K. Ensslin, C. Reichl, and W. Wegscheider, Phys. Rev. B **84**, 195322 (2011).

4. B. Hackens, F. Martins, T. Ouisse, H. Sellier, S. Bollaert, X. Wallart, A. Cappy, J. Chevrier, V. Bayot, and S. Huant, Nature Phys. **2**, 826 (2006).

5. A. Pioda, S. Kicin, T. Ihn, M. Sigrist, A. Fuhrer, K. Ensslin, A. Weichselbaum, S. E. Ulloa, M. Reinwald, and W. Wegscheider, Phys. Rev. Lett. **93**, 216801 (2004).

6. A. E. Gildemeister, T. Ihn, M. Sigrist, K. Ensslin, D. C. Driscoll, and A. C. Gossard, Phys. Rev. B **75**, 195338 (2007).

7. M. Huefner, B. Kueng, S. Schnez, K. Ensslin, T. Ihn, M. Reinwald, and M. Reinwald, Phys. Rev. B **83**, 235326 (2011).

8. S. Schnez, J. Güttinger, M. Huefner, Ch. Stampfer, K. Ensslin, and Th. Ihn, Phys. Rev. B **82**, 165445 (2010).

9. S. Schnez, J. Güttinger, M. Huefner, Ch. Stampfer, K. Ensslin, and Th. Ihn, arXiv:1005.2024.

10. M. Bockrat, W. Liang, D. Bozovic, J. H. Hafner, Ch. M. Lieber, M. Tinkham, and H. Park, Science **291**, 283 (2001).

11. M. T. Woodside and P. L. McEuen, Science **296**, 1098 (2002).

12. A. A. Zhukov and G. Finkelstein, Pis'ma Zh. Eksp. Teor. Fiz. **89**, 212 (2009).

13. A. C. Bleszynski, F. A. Zwanenburg, R. M. Westervelt, A. L. Roest, E. P. A. M. Bakkers, and L. P. Kouwenhoven, Nano Lett. **7**, 2559 (2005).

14. A. A. Zhukov, Ch. Volk, A. Winden, H. Hardtdegen, and Th. Schäpers, Pis'ma Zh. Eksp. Teor. Fiz. **93**, 13 (2011).

15. S. Schnez, J. Güttinger, C. Stampfer, K. Ensslin, and T. Ihn, New J. Phys. **13**, 053013 (2011).

16. M. Akabori, K. Sladek, H. Hardtdegen, Th. Schäpers, and D. Grützmacher, J. Cryst. Growth **311**, 3813 (2009).

17. A. A. Zhukov, Instrum. Exp. Tech. **51**, 130 (2008).

18. I. M. Ruzin, V. Chandraseckhar, E. I. Levin, and L. I. Glazman, Phys. Rev. B **45**, 13469 (1992).

19. F. R. Waugh, M. J. Berry, D. J. Mar, R. M. Westervelt, K. L. Campman, and A. C. Gossard, Phys. Rev. Lett. **75**, 705 (1995).

20. W. G. van der Wiel, S. De Franceschi, J. M. Elzerman, T. Fujisawa, S. Tarucha, and L. P. Kouwenhoven, Rev. Mod. Phys. **75**, 1 (2003).

21. Yu. V. Nazarov, Physica B **189**, 57 (1993).